ACS EARTH AND SPACE CHEMISTRY

Article

Cite This: ACS Earth Space Chem. 2018, 2, 410−421

Evaluation of the New Capture Vaporizer for Aerosol Mass Spectrometers (AMS): Elemental Composition and Source Apportionment of Organic Aerosols (OA)

Weiwei Hu,[†,‡,#] Douglas A. Day,[†,‡] Pedro Campuzano-Jost,[†,‡] Benjamin A. Nault,[†,‡] Taehyun Park,[§] Taehyoung Lee,[§] Philip Croteau,[∥] Manjula R. Canagaratna,[∥] John T. Jayne,[∥] Douglas R. Worsnop,[∥] and Jose L. Jimenez*[,†,‡]

[†]Cooperative Institute for Research in the Environmental Sciences (CIRES), University of Colorado at Boulder, 216 UCB, Boulder, Colorado 80309, United States

[‡]Department of Chemistry and Biochemistry, University of Colorado at Boulder, 216 UCB, Boulder, Colorado 80309, United States

[§]Department of Environmental Science, Hankuk University of Foreign Studies, Yongin 449-791, South Korea

[∥]Aerodyne Research, Inc., Billerica, Massachusetts 01821, United States

Supporting Information

ABSTRACT: To reduce the quantification uncertainty of commercial aerosol mass spectrometers (AMS) and aerosol chemical speciation monitors (ACSM), a new capture vaporizer (CV) was recently built to replace the standard vaporizer (SV). A collection efficiency (CE) ∼ 1 in the CV AMS/ACSM has been demonstrated for ambient aerosols, but the CV also leads to increased thermal decomposition of the analytes because of longer residence time and vaporizer surface contact. This study reports on the performance of the CV for analyzing organic aerosol (OA) elemental composition and source apportionment, using both HR-ToF-AMS and ACSM for the first time. The methodology for obtaining elemental ratios from AMS spectra is updated to account for differences in OA fragmentation between the CV and SV. An artifact CO^+ signal is observed for some chemically reduced laboratory compounds. If that signal is included in elemental analysis, the O:C is substantial overestimated, while accurate results are observed if the anomalous CO^+ is ignored. The estimated uncertainty of O:C (H:C) of standard organic species with the CV-AMS is 23% (18%). Consistent time series of positive matrix factorization (PMF) factors and their fractions of total OA were found across the CV and SV in the three very different ambient data sets ranging from biogenic- to anthropogenic-dominated, indicating limited loss of source determination information despite the increased fragmentation. In some cases, bootstrap analysis of CV data sets shows higher uncertainty for the apportionment of total oxygenated OA (OOA) into different subtypes than that of the SV data set, which is potentially due to lower signal-to-noise at larger m/z from the increased thermal decomposition in the CV.

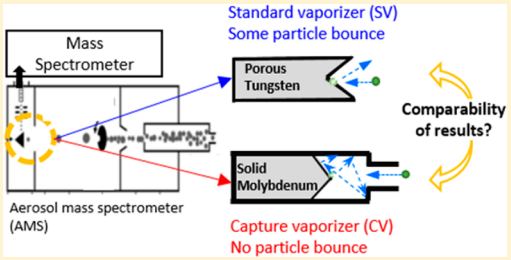

KEYWORDS: *Elemental composition, positive matrix factorization, PMF, thermal decomposition, particle bounce, SOAS study, KORUS-AQ study*

Downloaded via HANKUK UNIV OF FOREIGN STUDIES on July 5, 2018 at 01:56:51 (UTC).
See https://pubs.acs.org/sharingguidelines for options on how to legitimately share published articles.

1. INTRODUCTION

Aerosol mass spectrometer (AMS) or aerosol chemical speciation monitor (ACSM) instruments, which have been commercialized by Aerodyne Research Inc. (ARI), are widely used to quantify organic aerosols (OA) with a time resolution of seconds to minutes.[1−4] Analysis of the time variation of AMS/ACSM OA mass spectra with factor analysis methods (e.g., positive matrix factorization, PMF) has been widely used to investigate various sources and aging of OA and to help improve our understanding of primary emissions and secondary formation of OA.[5−10] The AMS is also capable of quantifying the elemental composition of OA, including atomic O:C and H:C.[11,12] Elemental analysis results have been used to investigate the chemical evolution of OA,[13−16] to quantify the conversion between organic carbon (OC) and OA,[12,17] and to constrain and improve model results.[18−22]

Almost all the currently operating AMS instruments use the standard vaporizer (SV), which has an open inverted cone structure and porous tungsten surface (Figure S1a). Some fraction of the solid particles impacting the SV can bounce, requiring the use of a collection efficiency (CE) correction (e.g., ∼0.2−0.5 for $(NH_4)_2SO_4$).[23,24] Typically ambient aerosol CE values vary between 0.5 and 1 depending on the chemical composition and phase of the aerosol.[23] CE is a major contributor to quantification uncertainty of aerosols in the AMS, as addressed in the Supporting Information (file jgrd15378-sup-0003-txts01.pdf)

Received: January 5, 2018
Revised: February 28, 2018
Accepted: March 2, 2018
Published: March 2, 2018

© 2018 American Chemical Society

DOI: 10.1021/acsearthspacechem.8b00002
ACS Earth Space Chem. 2018, 2, 410−421

of Bahreini et al.[25] Because of this limitation, a capture vaporizer (CV), with a narrow entrance and a trapping "cage" (Figure S1),[26] has recently been demonstrated to reduce particle bounce.

Recently, experimental results showed CE ~ 1 for CV-AMS analysis with ambient total and inorganic aerosols,[27] and improved CE for laboratory aerosols.[28,29] Increased mass spectral fragmentation was also observed for both inorganic and organic aerosols with the CV.[28−30] This shift in fragmentation pattern is thought to be due to increased thermal decomposition of neutral and/or increased fragmentation of ions with more internal energy, due to the additional residence time and hot surface collisions experienced by vaporized molecules in the CV. The increased decomposition has been found for all types of OA regardless of varied oxidation level or composition complexity in the CV, although its relative impact is smallest for ambient aerosols.[30] Given these changes in OA detection, it is important to evaluate whether the calibration parameters for elemental composition from SV OA mass spectra need to be updated for the CV. There is also a need to evaluate whether factor analysis capabilities routinely used for aerosol source apportionment are maintained with the CV. This manuscript describes multiple laboratory and field studies that use parallel deployments of SV- and CV-AMS instruments to address these questions. For reference, all the abbreviations and acronyms used in this study are explained in the "ABBREVIATION/GLOSSARY/NOMENCLATURE" section of this paper.

2. EXPERIMENT AND INSTRUMENTATION

2.1. Laboratory and Field Experiments. *Laboratory Studies.* Particles of pure organic compound standards were generated with three methods:

(1) Atomization, where analytes are dissolved into a suitable solvent based on their polarity and corresponding particles are generated with an atomizer (model: 3076, TSI); Hexane (purity >95%, Sigma-Aldrich), isopropanol (>99.5%, Sigma-Aldrich), and water (Milli-Q) were used as solvent;
(2) Laser ablation method, where a solution or OA liquid was dropped on a glass or thin-layer chromatography (TLC) plate and dried, then particles were generated using the focused output of a Nd: YAG laser (212.8 nm) through irradiation of the solid material on the plates;[31−33]
(3) Evaporation−condensation method,[34] where particles were generated on the basis of vapor recondensation by mixing of cooler air after being evaporated in a heated glass flask. In this study, particles from 21 different pure organic compounds were analyzed. Detailed information on each compound, such as name, formula, aerosol generation method, and carrier gas, is listed in Table S1.

Field Studies. Data from three field studies were used. (1) The Southern Oxidation Aerosol Study (SOAS) was carried out at a ground site in a pollution-influenced forest area in the Southeast US during the summer of 2013.[35] OA was strongly influenced by biogenic emissions.[36,37] (2) The KORean-United States Air Quality mission (KORUS-AQ, May-June, 2016) was an aircraft-based field campaign to investigate the factors controlling air quality in and around the Seoul Metropolitan Area; anthropogenic (vehicular and industrial) sources are important for this data set. Significant contribution from aged long-range transport sources was also expected. OA data from several flights (Research Flights, RF 05, 12, 18), which are representative of the range of conditions encountered during KORUS-AQ, are used in this study. (3) The Billerica study (September, 2012) was conducted on the campus of ARI, located in a suburb of Boston, MA (U.S.A.), and, hence, is expected to be affected by urban pollution and regional aged aerosols.

2.2. AMS/ACSM. Two high-resolution time-of-flight AMSs (HR-ToF-AMSs), equipped with a SV and CV, respectively, were deployed in all the laboratory studies. In the SOAS study, an HR-ToF-AMS with the SV was used for the entire campaign, while a second AMS equipped the CV was used with a compact time-of-flight AMS (C-ToF-AMS, m/Δm: ~ 750)[38] for most of the campaign, and with an HR-ToF MS for a few days (June 7−10). In the KORUS-AQ study, two HR-ToF-AMSs, outfitted with a CV (Hankuk University AMS) and SV (University of Colorado aircraft AMS), respectively, were run alongside on the aircraft platform (NASA DC8) with different sampling lines for most of time (occasionally, two AMSs both sampled from the sample inlet). For the Billerica study, two ACSMs,[4] equipped with a SV and CV, were used. This study allows investigating the performance of OA analysis with the CV in the ACSM, which uses a different measurement protocol (e.g., different aerosol/background subtraction method and sequence), which could affect OA analysis.[4,10]

AMS calibrations of ionization efficiency (IE) were conducted before each set of experiments in the laboratory or every few days in the case of the field studies. Particle velocity/sizing calibration was determined before the experiment or in the middle of the campaign when necessary. Details on the setup of the instruments are shown in Figure S1, and the detailed calibration protocol of the AMS was reported in Hu et al.[27,28]

2.3. Elemental Analysis Methods. Two elemental analysis methods were applied for the SV-AMS: the Aiken method[12,39] and the Canagaratna Improved-Ambient (C-IA) method.[11] Two different variants of the Aiken method were used. In the "Aiken explicit (A-E) method", calibration parameters were applied to the elemental ratios determined by fitting all the major organic peaks of pure standard species when CO^+ and H_2O^+ ions (arising from OA) could be clearly resolved in the spectrum, and no residual particulate water was present.[39] Argon (Ar) was used as the carrier gas instead of air in these experiments in order to reduce interference from the large N_2^+ signal for CO^+ and tight RH control was used to reduce the interference of particle water on molecular water fragments. The "Aiken ambient (A-A) method" was applied to the ambient aerosol measurements, where CO^+ and H_2O^+ from OA are very difficult to quantify directly due to interferences from ambient air that produce N_2^+ and other sources of H_2O^+. In this method, CO^+ ions are estimated based on the measured CO_2^+ ion (assuming CO^+/CO_2^+=1), and similarly for H_2O^+ (H_2O^+/CO_2^+ = 0.225), HO^+ (HO^+/H_2O^+ = 0.25), and O^+ (O^+/H_2O^+ = 0.04) ions.[12] The A-A method uses the same calibration parameters of O:C and H:C as A-E method. Canagaratna et al.[11] showed that the elemental ratios of multifunctional oxidized standards estimated from the A-A method were biased low, while A-E method still performed well. Thus, Canagaratna et al.[11] introduced the C-IA method to reduce the errors when analyzing such compounds.

2.4. PMF Source Apportionment. Unconstrained PMF analysis was performed on the time series of the OA spectral matrix measured by the SV and CV from the SOAS, KORUS-AQ and Billerica studies.[5] For the SOAS and Billerica field studies, PMF (PET, PMF Evaluation Tool, which is PMF analysis interface software, version 2.04−2.08 in Igor 6.37) was performed on unit mass resolution OA matrices (UMR, m/z 12−120

DOI: 10.1021/acsearthspacechem.8b00002
ACS Earth Space Chem. 2018, 2, 410−421

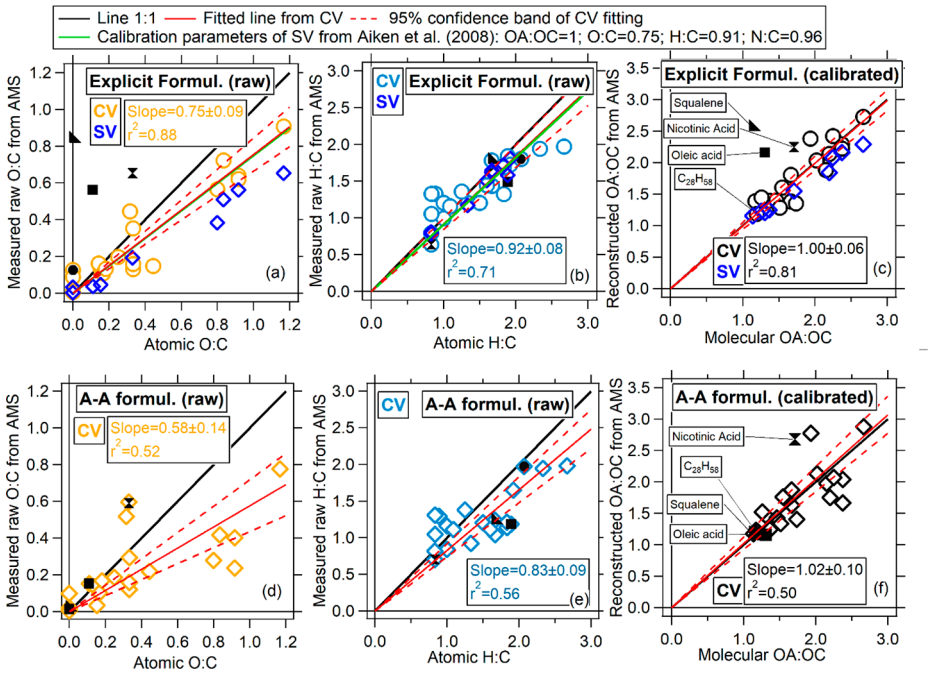

Figure 1. Scatter plots of elemental ratios from HR-ToF-AMS spectra of atomized standards vs the nominal atomic ratios in the CV. In the upper panel (a−c), the reported raw elemental ratios use the explicit formulation. The CO^+ and H_2O^+ ions are directly measured and included in the reported ratios. In the lower panel (d−f), Aiken ambient (A-A) fragmentation table, which constrains CO^+ and H_2O^+ abundance based on CO_2^+ ions (CO^+/CO_2^+ = 1; H_2O^+/CO_2^+ = 0.225), was applied. In Figure 1a,b and d,e, the direct measurements are shown; that is, no calibration parameters are applied to the measured O:C and H:C ratios. For OA:OC ratios in panels c and f, they were reconstructed on the basis of the calibrated O:C and H:C ratio (= 16*O + 1*H + 14*N + 12*C)/12). In this equation, the calibrated O:C and H:C for each species were obtained based on raw O:C dividing by the regression slope in Figure 1a (and Figure 1d) and Figure 1b (and Figure 1e), respectively. The elemental ratio values of several species for the SV (in blue) with explicit formulation are also shown, and the calibration slopes obtained from Aiken method[12] have also been included (green lines). The uncertainty of regression ratio of OA:OC is 9%. The detailed information on the name of those compounds and estimation method can be found in Tables S1,S2.

for SOAS and m/z 12−100 for Billerica) from the SV and CV. Additionally, for the SOAS data, PMF was performed on the HR data set in the SV (m/z 12−100) for comparison. For the KORUS-AQ study, HR spectral matrixes for both vaporizers were used for PMF analysis (PET 2.08 in Igor 6.37). For all the studies, m/z 16, 17, 18, and 28 were constrained on the basis of the intensity of the m/z 44 peak (CO_2^+ for HR).[12] A square root of 5 (= 2.23, due to 4 other ions being directly calculated from m/z 44 in the fragmentation table) was applied to down-weight those peaks in the SV and CV because of their redundant information.[5]

3. RESULTS AND DISCUSSION

3.1. Determination of Elemental Composition with the CV. *3.1.1. O:C and H:C Ratios: Explicit Method.* Elemental composition, often measured by AMS, i.e., O:C, H:C, and OA:OC (OA:OC = organic aerosol-to-organic carbon mass ratio, sometimes referred to as OM:OC), has been widely used to investigate the chemical evolution of OA (e.g., Jimenez et al.,[13] Kroll et al.,[14] and Heald et al.[15]). The elemental ratios measured with the CV are evaluated in this study for the first time with pure standard species. Detailed information on those standard species, such as name and formula, is given in Table S1,S2.

Figure 1 shows the comparison between measured elemental ratios in the CV and nominal molecular/atomic ratios. Because the organic-derived CO^+ and H_2O^+ contributions from the organic species can be explicitly measured for pure standards under an Ar carrier gas (or N_2 and air under high OA concentration), the measured values are used directly (without calibration factors) to calculate the elemental ratios measured by the CV. Good correlation between measured O:C (slope = 0.75; r^2 = 0.88) and nominal values is observed, as well as for H:C (slope = 0.92; r^2 = 0.71), as shown in Figure 1a,b.

The measured elemental ratios from squalene, oleic acid, octacosane, and nicotinic acid fall out of the regression line, which is mainly caused by artificially high CO^+ and H_2O^+ fractions of total OA signal (10−40%) in their spectra, which might be produced through chemical reactions between the sampled OA and residues on the vaporizer surfaces.[30] When the CO^+ and H_2O^+ of these four species are estimated on the basis of the A-A fragmentation table (CO^+/CO_2^+ = 1; H_2O^+/CO_2^+ = 0.225), the resulting elemental ratios are much closer to the expected values (Figure 1d,e). These four species are not taken into account for the final regression. Except for these four species, there are no obvious high biases for CO^+ and H_2O^+ for other species. A comparison of organic CO^+/CO_2^+ and organic H_2O^+/CO_2^+ ratios for different standard OA species between the CV and SV are listed in Table S3.

The CV elemental ratios obtained from the direct measurements (without calibration factors) are similar to those obtained for the SV cosampled in this study, which indicates that the increased fragmentation in the CV does not result in a loss of information about elemental composition. The regression slopes (i.e., calibration factors) in the CV (0.75 for O:C and 0.92 for H:C) are also similar to the original SV estimates for the A-E method (0.75 for O:C and 0.91 for H:C) in previous calibrations.[12] The uncertainty, defined as the average absolute value of the relative error of each data point with respect to the

DOI: 10.1021/acsearthspacechem.8b00002
ACS Earth Space Chem. 2018, 2, 410−421

regression line is 23% for O:C and 18% for H:C, which is also similar to the values (31% and 10%, respectively) from Aiken et al.[12,39] We propose to use the regression slope of 0.75 for O:C ratio and 0.92 for H:C as calibration factors for the elemental ratios measured in the CV for the explicit method (i.e. when the organic contribution to H_2O^+ and CO^+ can be directly and accurately quantified). However, the appearance of artifact signal at CO^+ especially for chemically reduced species needs to be evaluated, for example, with the beam alternation experiments discussed by Hu et al.[30]

3.1.2. O:C and H:C Ratios: Ambient Method. CO^+ and the organic contribution to H_2O^+ are very difficult to quantify directly in most ambient studies even with HR data, and especially at high time resolution. They are nearly impossible to quantify for ambient UMR data from the ACSM. Thus, an "ambient" quantification method for OA elemental composition is needed for these situations in which the "explicit" method just described above cannot be applied, by estimating CO^+ and H_2O^+ using a fragmentation table.[11,12]

In the SV, A-A fragmentation table (CO^+/CO_2^+ = 1; H_2O^+/CO_2^+ = 0.225) was used. In the following, CO^+/CO_2^+ and H_2O^+/CO_2^+ ratio in the ambient aerosols between the SV and CV are examined to evaluate if A-A fragmentation table is also suitable for the CV. An artifact CO^+ enhancement in the CV has not been observed for ambient aerosols so far, probably due to the prompt thermal decomposition process of ambient aerosols, and possibly the fact that the campaigns analyzed here do not include very high contributions from chemically reduced components such as hydrocarbon-like OA (HOA).[30] It indicates the O:C and H:C ratio for ambient aerosols should not be biased due to this vaporizer artifact. In addition, elemental ratios of several standard species between Ar and air systems were compared in this study (Figure S2). We did not find systematic differences of elemental ratios between Air and Ar in either the SV or CV, suggesting oxygen in the carrier gas does not introduce bias in the CV elemental ratios.

During the SOAS and KORUS-AQ study, an average CO^+/CO_2^+ ratio of 1.30 ± 0.24 was obtained by averaging the measured CO^+ vs CO_2^+,[30] which is similar to CO^+/CO_2^+ of 1.20 ± 0.21 for the SV, and within the range of values observed for the SV in past studies.[11] We also compared the measured H_2O^+ vs CO_2^+ in the SOAS study. After subtracting background H_2O^+ (calculated on the basis of filter data) and sulfate H_2O^+ (calculated on the basis of the measured ambient sulfate multiplying measured H_2O^+/sulfate mass ratio when pure sulfate was sampled during calibrations) from measured H_2O^+ signal in AMS, H_2O^+/CO_2^+ showed similar ratios in the SV and CV (~1). We cannot exclude that some particulate H_2O^+ remains in ambient aerosols in this calculation because the RH was only dried below 30−40%, and a fraction of the particulate water is tightly bound to particles. The measured closed signal ratio of O^+/H_2O^+ and HO^+/H_2O^+ in the CV are ~0.22−0.23 and ~0.03 during the SOAS and KORUS-AQ field studies, respectively, which are similar to the values detected in the SV (~0.22 and ~0.04). The similarity of CO^+/CO_2^+ and H_2O^+/CO_2^+ ratios in difference mode (open minus closed signal), as well as HO^+/H_2O^+ and O^+/H_2O^+ in closed mode (beam closed signal), in the SV and CV when the same ambient particles were sampled suggests that using the default SV ambient fragmentation table for the CV may be appropriate.

We compared the elemental ratios for the standards using the traditional A-A fragmentation table (H_2O^+/CO_2^+ = 0.225 and CO^+/CO_2^+ = 1) in Figure 1d,e. Lower regression slope (0.58 for O:C and 0.83 for H:C) and coefficient of determination (r^2 = 0.52 and 0.56, respectively) than the values for the explicit method (slope = 0.75 of O:C and 0.92 of H:C; r^2 = 0.88 and 0.71, respectively) were found. This is not surprising because there is variability of CO^+/CO_2^+ (also H_2O^+/CO_2^+) ratios across different compounds (Table S3). In fact, the lower regression slopes when A-A fragmentation table (Figure 1d,e) applied (Figure 1a,b) are also found for the SV.[11]

It is possible that different CO^+/CO_2^+ and H_2O^+/CO_2^+ ratios other than those used in the A-A fragmentation table could produce better results for CV data. This is explored in Figure S3. In summary, no clear improvement is found for other values, and the results with the A-A default setting are within the optimum solution region, suggesting it should be reasonable to use A-A fragmentation table values in the CV.

3.1.3. O:C and H:C Ratios: Application to Ambient Data. Next, we check if the calibration parameters derived with standard OA above are suitable for ambient measurements. O:C and H:C ratios for the SV, quantified using the C-IA method and calibration parameters,[11] were used as the standard reference to which results for measured O:C and H:C ratios for the CV can be compared to. We first apply the A-A fragmentation table (CO^+/CO_2^+ = 1 and H_2O^+/CO_2^+ = 0.225) and the calibration slopes derived from OA standards (0.58 for O:C and 0.83 for H:C). After applying these calibration parameters to the ambient OA, we found an overestimation for O:C (slope = 1.24−1.27) and underestimation for H:C (0.82−0.88) compared to the SV results, as shown in Figure S4a,b. This inconsistency suggests that the calibration parameters derived for OA standards here are not suitable for ambient OA. This may be caused by the limitations of the standard OA data set used, which may not be sufficient to capture the variability of ambient OA. To address this question, we recommend a further calibration study with a greatly expanded standard OA data set including more different types of OA (e.g., acids, peroxides, polyols).

Alternative calibration parameters can be derived by comparing the raw O:C and H:C ratios measured from the CV directly with the values from the SV for ambient data. The comparisons of ambient O:C and H:C between the CV and SV during the SOAS and KORUS-AQ studies are shown in Figure 2 and Figure 3, respectively. Using the A-A fragmentation table with CV data set, good correlation of O:C and H:C ratio between the CV and SV are observed, for both the biogenic emission dominated SOAS study (R ~ 0.5−0.9, Figure 2) and anthropogenic emission dominated KORUS-AQ study (R ~ 0.8−0.9, Figure 3). The obtained regression slopes from SOAS study (O:C slope = 0.72; H:C slope = 0.74) are similar to these from the KORUS-AQ studies (O:C slope = 0.74; H:C slope = 0.69). Average slopes of O:C (0.73) and H:C (0.72) for the SOAS and KORUS-AQ studies can be used as initial calibration parameters for ambient data in the CV, until more detailed laboratory calibrations can be conducted. After applying those calibration parameters, consistent variation of O:C and H:C vs corresponding elemental ratios from SV were observed (Figure 2e and Figure 3e) with regression slopes of 0.98−1.01 and 0.95−1.03, respectively (Figure. S4c,d). Positive relationship between O:C vs f_{44} (= m/z 44/OA) and H:C vs f_{43} (= m/z 43/OA) ions in the SV has been reported in previous studies.[12,16] We also explored the relationships between O:C vs f_{44} and H:C vs f_{43} ions in the CV, as shown in Figure S5. Both field studies show consistent variations of elemental ratios versus their tracer fractions in OA in the CV. The fitting parameters in the CV, which is slightly different than the results in the SV, can be used to

DOI: 10.1021/acsearthspacechem.8b00002
ACS Earth Space Chem. 2018, 2, 410−421

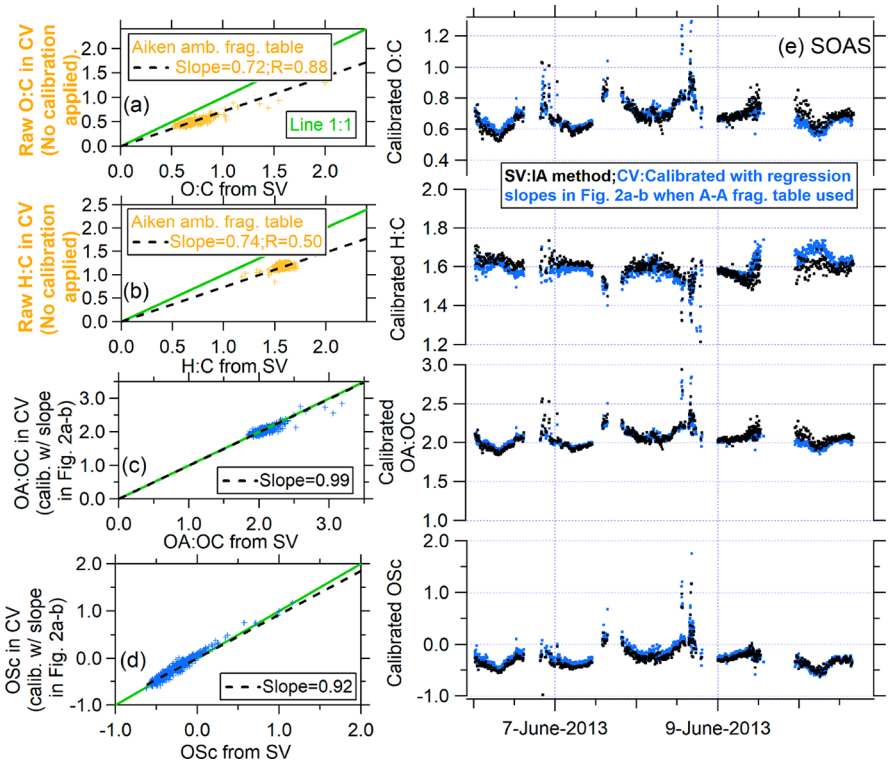

Figure 2. (a) Comparisons of scatter plots of (a) O:C, (b) H:C, (c) OA:OC, and (d) average carbon oxidation state (OSc = 2O:C−H:C) and (e) their time series between the CV and SV in HR-ToF-AMS, during the SOAS study. In Figure 2a,b, raw O:C and H:C measured by the CV were shown. The elemental ratios from the CV in Figure 2c,d and Figure 2e are calibrated with the parameters shown in Figure. 2a,b.[12] All the data from the SV are estimated on the basis of the C-IA method.[11]

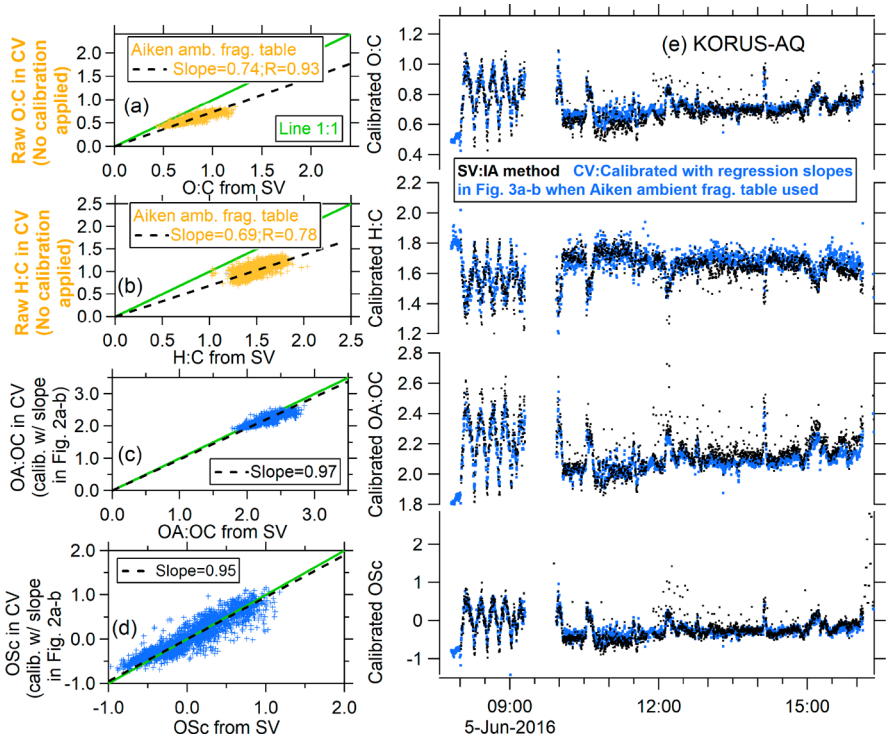

Figure 3. (a) Comparisons of scatter plots of (a) O:C, (b) H:C, (c) OA:OC, and (d) average carbon oxidation state (OSc = 2O:C−H:C) and (e) their time series between the CV and SV in HR-ToF-AMS, during the KORUS-AQ study. In Figure 3a,b, raw O:C and H:C measured by the CV were shown. The elemental ratios from the CV in Figure 3c,d and Figure 3e are calibrated with the parameters shown in Figure 3a,b.[12] All the data from the SV are estimated on the basis of the C-IA method.[11]

estimate rough elemental ratios based on f_{44} and f_{43}, for example, when only unit-resolution data is available.

We explored the impact of particle beam position on the CV (center vs edges) on OA parameters, because this experiment

DOI: 10.1021/acsearthspacechem.8b00002
ACS Earth Space Chem. 2018, 2, 410−421

Table 1. Recommended Calibration Parameters for O:C and H:C Ratios Measured by the CV with Calibration Parameters from the Aiken Method for the SV[12] Shown as a Reference[a]

	fragmentation table	O:C	H:C	N:C	reference
		standard OA			
SV: Aiken explicit method	fitted CO^+ and H_2O^+	0.75	0.91	0.96	12
CV: explicit method	fitted CO^+ and H_2O^+	0.75	0.92	N/A	this study
		ambient aerosols			
CV: A-A fragmentation table	CO^+/CO_2^+ = 1 H_2O^+/CO_2^+ = 0.225	0.73	0.72	N/A	this study

[a]For the explicit method, those parameters were obtained by comparing the directly measured O:C and H:C of standard organic compounds with their nominal values. For the ambient aerosols, those values are estimated on the basis of comparing the directly measured O:C and H:C in the CV with C-IA method calibrated elemental ratios measured in the SV.

was useful for inorganic species.[28] When the particle beam is aimed at the edge of the CV, the citric acid spectra recorded are more similar to the spectra from the SV because of the short residence time of particle with vaporizer surfaces (Figure S6).[30] Lower f_{44} and higher H:C were observed at the edges of the vaporizer, which is consistent with the lower thermal decomposition shown in previous studies. The O:C ratios are stable between the edge and center, suggesting that enhanced thermal decomposition might not lead to extra O loss in the CV.

In summary, we propose to use the parameters listed in Table 1 to calibrate the O:C and H:C ratios measured in the CV. We recommend the use of explicit formulation with calibration parameters of 0.75 for O:C and 0.92 for H:C for pure organic compounds measured in environments with negligible or quantifiable contributions from gas phase H_2O and CO_2. The presence of artifact CO^+ should be evaluated further for reduced compounds. The ambient fragmentation table (CO^+/CO_2^+ = 1; H_2O^+/CO_2^+ = 0.225) is recommended for ambient OA measurement with calibration parameters of 0.73 for O:C and 0.72 for H:C being used. An expanded effort with a larger data set to assess the CV calibration parameters for both ambient and laboratory studies is recommended.

3.1.4. N:C Ratios. For N:C ratios, the current data set is not large enough to obtain quantitative calibration parameters, but some trends become clear nevertheless. Nicotinic acid ($C_6H_5NO_2$, N:C = 0.17) and 1,2-bis(4-pyridyl)ethylene ($C_{12}H_{10}N_2$, N:C = 0.17) particles were sampled simultaneously in the SV and CV. Comparable N:C ratios were observed (0.12 and 0.08, respectively, in the SV versus 0.09 and 0.08, respectively, in the CV); both are lower than the nominal species values (0.17). For ambient aerosols, since V-mode ($m/\Delta m$ = ~2000−3000) was used for the CV in both field studies discussed here, the AMS resolution was not high enough to obtain an accurate separation of $C_xH_yN_p^+$ and $C_xH_yN_pO_z^+$ ions vs other organic ions ($C_xH_y^+$, $C_xH_yO_z^+$),[40] especially accounting for their low abundance in both ambient studies reported here (atomic N:C usually <0.05). Thus, a thorough investigation with a greater data set of nitrogen-containing standard compounds, ideally taking advantage of the new higher resolution LToF-AMS in both the SV and CV is recommended for evaluating the quantification of N:C ratios.[11,12,39]

3.1.5. OA:OC and OSc. After calibrating O:C and H:C ratios for the A-E and A-A formulation, the OA:OC ratios from the CV show good agreement with their nominal values for pure chemical compounds (slope = 0.99, Figure 1c,f), and with estimated ambient OA:OC from the SV (slope = 0.97−0.99, Figure 2c and Figure 3c), respectively. The regression slopes for ambient aerosols are also well within the 6% uncertainty estimated in Aiken method[12,39] and 9% for the C-IA method.[11] Consistent values and variation of approximate average carbon oxidation state (OSc, = 2*O:C−H:C)[14] between the SV and CV in the two ambient studies are also found (Figures 2 and 3).

3.2. Source Apportionment of OA. PMF[41,42] is a factor analysis or receptor model based on the assumption that a measured data set conforms to a mass-balance of a number of time-invariant source/component profiles varying in concentration over the time period.[5−8] The resulting matrix of concentrations vs time can be used to estimate the component profiles and their contributions in time. PMF analysis is widely used with OA measurements from the AMS to investigate the primary emission and secondary formation of aerosols in ambient and chamber studies.[5] Here, we examine the ability of PMF to separate OA components with CV-AMS data by comparing with PMF results from the colocated SV-AMS.

PMF was run without constraints using the PMF Evaluation Panel (PET 2.04−2.08) within Igor Pro.[5] The optimum PMF solution of each study for both the SV and CV was determined independently following the procedures of Ulbrich et al.,[5] using Q/Q_{exp}, comparison with external OA spectra, and comparison of PMF factor time series with those of tracers (e.g., sulfate, nitrate, black carbon, etc.). While a solution with the rotational parameter FPEAK = 0 was selected for most of studies, a FPEAK = 0.6 was chosen for the CV during KORUS-AQ, due to better spectra separation and stronger correlation with external tracers than FPEAK = 0 (Figures S7,S8). Finally, the source apportionment results between the CV and SV from three field studies are compared in Figures 4−6.

For the SOAS study, a four-factor solution from unconstrained PMF analysis for the SV and CV is compared. The factors are (i) Isoprene-epoxydiols derived SOA (IEPOX-SOA), which is mainly formed through oxidation of isoprene under low NOx conditions in the presence of acidic aerosols;[36,43] (ii) more oxidized OOA (MO-OOA), which represents aged SOA and has a good correlation with the long-lived VOCs such as acetone (R = 0.8); (iii) less-oxidized OOAI (LO-OOAI), which has a good correlation with organic nitrate (R = 0.8) and is suggestive of being formed through the oxidation of biogenic-emitted monoterpene with O_3 and NO_3 radicals;[37,44] and, (iv) less-oxidized OOAII, which correlates better with benzene (R = 0.7). This factor is strongly influenced by anthropogenic urban plumes. Biomass burning OA (BBOA) cannot be resolved in unconstrained PMF analysis during the SOAS study, due to its small contribution to total OA (<5%) during the period analyzed here.[5] An average of 3% BBOA/total OA was obtained in the SV data set by constraining the BBOA spectrum averaged from various chamber and field studies in the constrained PMF method, as implemented in the multilinear engine (ME-2, SoFi v6.1) software.[6,45] Unlike for the SV, the AMS spectral database

DOI: 10.1021/acsearthspacechem.8b00002
ACS Earth Space Chem. 2018, 2, 410−421

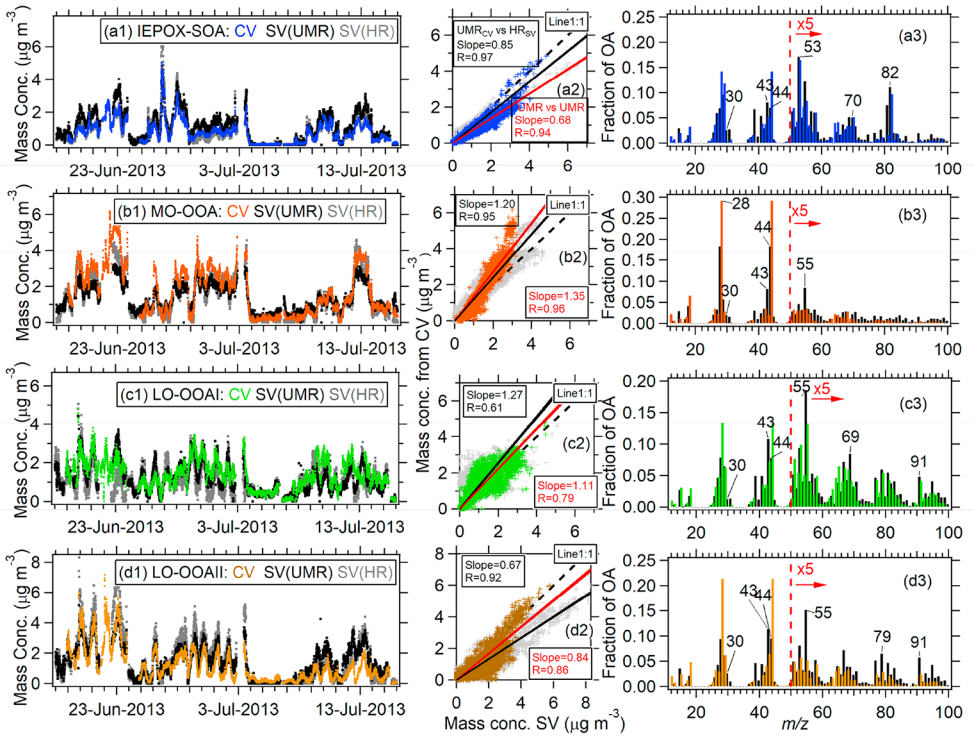

Figure 4. Comparisons of time series, scatter plot, and spectra of PMF factors: (a) IEPOX-SOA, (b) MO-OOA, (c) LO-OOAI (biogenic origins) and (d) LO-OOAII (anthropogenic origins), from the CV and SV during the SOAS study. In SOAS, the linear regression slope of total OA concentration between the SV and CV is around 0.9. For a fair comparison of PMF source apportionment ability, the regression slope of total OA between the SV and CV is forced to be 1 by multiplying the OA matrix of the SV by a factor of 1.1.

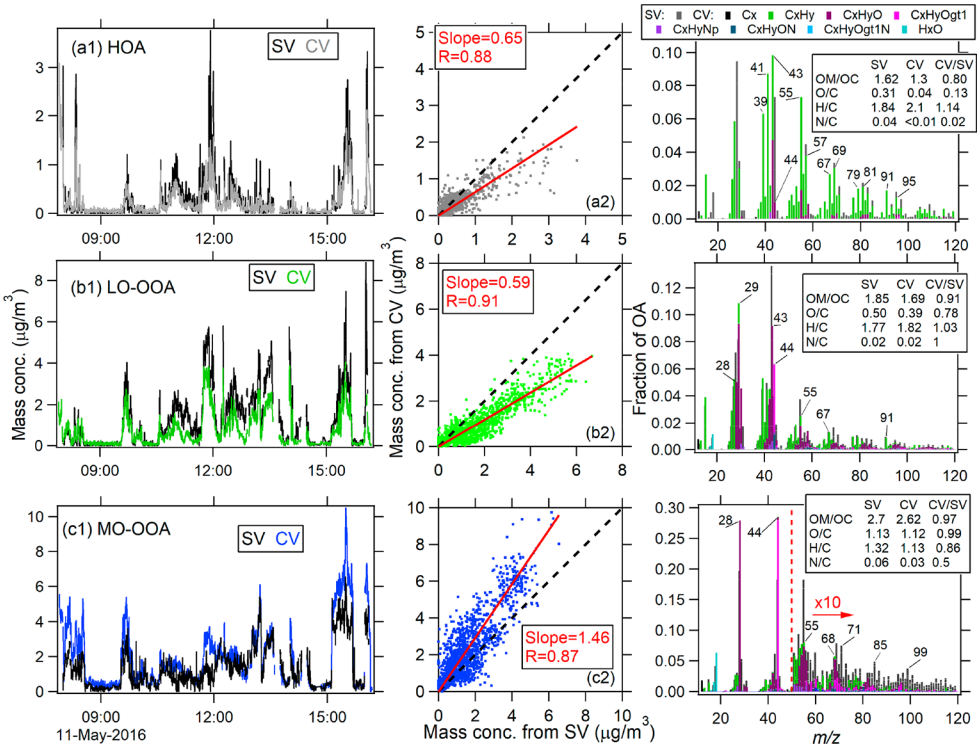

Figure 5. Comparisons of time series, scatter plots, and spectra of PMF factors: (a) HOA; (b) LO-OOA and (c) MO-OOA, for the SV and CV from the KORUS-AQ (RF05) study. Elemental ratio comparisons are also included. The regression slope of total OA between the SV and CV for this KORUS-AQ flight (RF-05) is ~1.

for the CV-AMS is still very limited (e.g., lacking examples of ambient and chamber BBOA spectra). Thus, comparisons based on constrained PMF for both vaporizers are not yet possible. A spectral database for AMS measurements with the CV[46] has been recently established at http://cires1.colorado.edu/jimenez-group/AMSsd_CV/.

DOI: 10.1021/acsearthspacechem.8b00002
ACS Earth Space Chem. 2018, 2, 410−421

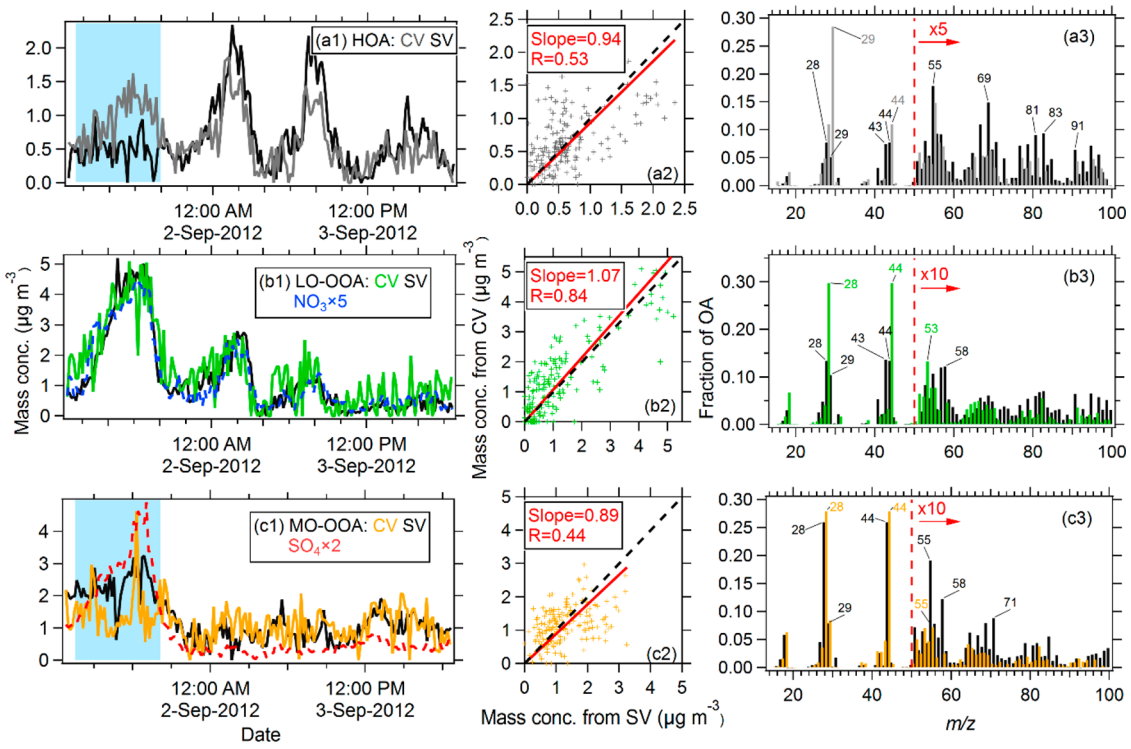

Figure 6. Comparisons of time series, scatter plots, and spectra of PMF factors: (a) HOA, (b) LO-OOA, and (c) MO-OOA, for the CV and SV during the Billerica study. The regression slope of total OA between the SV and CV in the Billerica study is ~1.

Good comparisons for the factor time series between the SV and CV is found (with R between 0.80 and 0.90 for UMR vs UMR; R between 0.61 and 0.97 for HR vs UMR), as shown in Figure 4. An improved regression slope and R of LO-OOAI and LO-OOAII in the comparison of UMR vs UMR (LO-OOAI: slope = 1.16; R = 0.80; LO-OOII: slope = 0.88, R = 0.86) compared to HR vs UMR (slope = 1.32; R = 0.61; slope = 0.70, R = 0.90) is observed. For all factors, m/z 44 and its related ions (e.g., CO^+ and H_2O^+) show higher abundances in the CV than the SV, consistent with the enhanced f_{44} in CV during SOAS.[30] f_{44} in all CV PMF factors is still positively correlated with f_{44} in the SV factor. This suggests that the variation of f_{44} in different PMF factors from the CV is still distinct, despite the larger values (Figure S9). Characteristic tracer ions (e.g., m/z 82 and m/z 53 for IEPOX-SOA and m/z 91 for LO-OOAII and I) also appear in their respective CV PMF factor spectra similar to the corresponding PMF factors from the SV. Meanwhile, the MO-OOA factor is the most oxidized factor for both the CV and SV.

For the KORUS-AQ study, three PMF factors, including hydrocarbon-like OA (HOA, correlated with black carbon, $R \approx 0.8$), less-oxidized OA (LO-OOA, correlated well with aerosol nitrate and formaldehyde, $R > 0.84$) and more-oxidized OA (MO-OOA, correlated with sulfate, $R > 0.7$) are resolved, as shown in Figure 5. Good correlation coefficients of all the time series of PMF factors between the SV and CV ($R > 0.87$) are found in the KORUS-AQ study. For the Billerica study, three PMF factors were resolved. Good correlation of LO-OOA (R = 0.84) and moderate correlation of MO-OOA (R = 0.44) and HOA (R = 0.53) between the CV and SV are found (Figure 6). The slightly poorer correlation of HOA and MO-OOA in the Billerica study is mainly caused by some differences in the time series in the early comparison period (light blue background in Figure 6) and may be influenced by the very short time period and thus limited number of data points available for PMF comparison (3.5 days with ~180 points, while a week or longer period with more points, e.g., > 1000, is preferred) and limited signal-to-noise of the ACSM. Consistent with SOAS, prominent peaks at m/z 44 and m/z 28 are observed in the spectra of almost all PMF factors from the CV in both the Billerica and KORUS-AQ studies (except for HOA in KORUS-AQ), while ions above m/z 44 are less abundant in the CV compared to the SV. Similar to the SV, the HOA factor from the CV in KORUS-AQ and Billerica also shows much higher $f_{m/z}$ at m/z > 50 than the other OOA factors. Positive correlation of the O:C and H:C ratios of the respective PMF factors are also observed in KORUS-AQ study (Figure S9).

The average fractions of total OA for each PMF factor of the total OA are shown in Figure 7. In all three studies, the fraction of each factor for the SV vs CV are reasonably consistent with each other. The only significant difference observed is the higher MO-OOA (37%) for the CV vs SV in KORUS-AQ. However, a consistent overestimation of MO-OOA is not observed across the different studies because the values are more similar for SOAS and actually lower MO-OOA for the CV than SV in the Billerica study. It is well-known that the separation of different types of OOA is the most difficult and uncertain aspect of PMF of AMS data (e.g., Ulbrich et al.),[5] so these observations are not surprising. The factors that are more chemically and spectrally distinct (e.g., HOA and IEPOX-SOA) compare well across CV and SV. The reasons causing the slight differences of PMF factor separation between the CV and SV are unclear and may be influenced by different signal-to-noise (S/N) ratios due to different relative instrument sensitivities (not related to the vaporizers), as shown in Figure S10. The bootstrap calculation shows lower uncertainty of PMF deconvolution in the CV than the SV for the SOAS study, higher uncertainties for PMF deconvolution in the CV than the SV for the KORUS-AQ and Billerica studies (especially for the separation

DOI: 10.1021/acsearthspacechem.8b00002
ACS Earth Space Chem. 2018, 2, 410−421

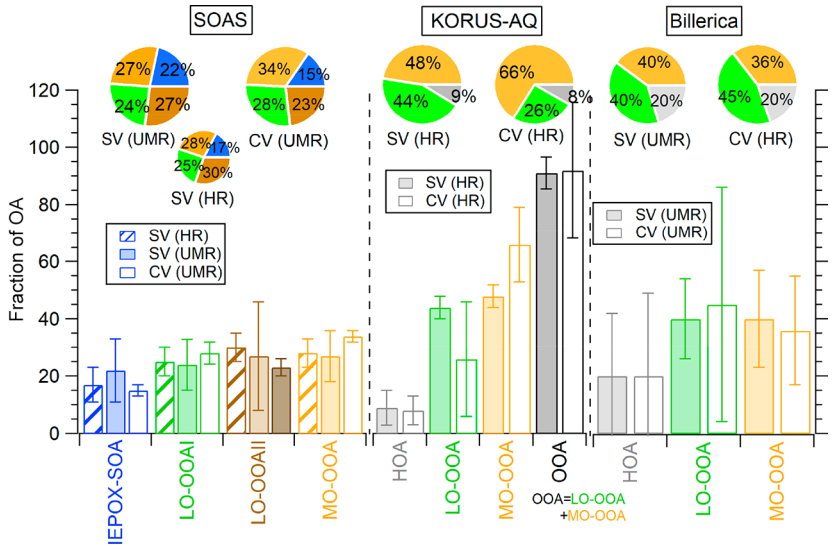

Figure 7. Fraction of each PMF factor in total OA during the SOAS, Billerica, and KORUS-AQ studies. Pie charts of PMF factor contributions for the CV and SV are also shown. The uncertainty bar of each PMF factor is calculated based on bootstrapping analysis (Table S4).

of OOA factors), as shown in Figure 7. Despite the slightly different PMF factor separation, the linear correlation of PMF factors between the SV and CV, comparable concentrations, and the fact that characteristic ions are still observed in each PMF factor indicate that the PMF analysis with the CV is similarly useful to that with the SV.

4. CONCLUSIONS

In this study, we have examined the performance of the CV in the AMS for OA elemental analysis and source/component apportionment using multiple pure OA standard compounds and ambient OA. Calibration parameters for O:C and H:C ratio in A-E (O:C of 0.75 and H:C of 0.92) and A-A formulations are derived on the basis of comparing the measured elemental ratio of pure organic species in the CV vs their theoretical values. Calibration parameters for ambient OA (O:C of 0.73 and H:C of 0.72) are also recommended based on comparing the measured elemental ratios of ambient aerosols vs those estimated from C-IA method in the SV. We recommend the use O:C of 0.75 and H:C of 0.92 to calibrate elemental ratios from the CV when H_2O^+ and CO_2^+ can be accurately assessed, and to apply O:C of 0.73 and H:C of 0.72 as calibration parameters for ambient OA measured with the CV. A few outliers (specifically oleic acid, squalene, and nicotinic acid) were found to have artificially high O:C ratios largely due to unusually high CO^+ and H_2O^+ ion intensity. After calibration, good agreement of the measured OA:OC and OSc between the CV and SV was obtained. No effect of oxygen from the carrier gas was observed. Evaluating the CV calibration and CO^+/CO_2^+ and H_2O^+/CO_2^+ ratios with additional standard compounds and other types of ambient aerosols (e.g., biomass burning OA) in future studies is recommended.

PMF results from the CV data sets show good agreement with those from the SV in three field studies in very different environments, including an aircraft study (SOAS, Billerica, and KORUS-AQ), indicating that PMF analysis of CV-AMS is similarly useful as for SV-AMS. In some cases (e.g., same type AMSs equipped with the CV and SV being compared), the chosen solutions and the bootstrap analysis shows higher uncertainty for the apportionment of OOA subtypes in the CV than the SV, which might be due to the low signal-to-noise at larger m/z from the increased thermal decomposition in the CV. With wider use of CV in the future, a larger database of representative spectra from different types of OA can be obtained, which will help guide other source apportionment analyses (e.g., chemical mass balance (CMB) and constrained PMF analysis (ME-2)) using the CV, of particular importance for ACSM measurements where the PMF rotational ambiguity is typically larger.

■ ASSOCIATED CONTENT

Supporting Information

The Supporting Information is available free of charge on the ACS Publications website at DOI: 10.1021/acsearthspacechem.8b00002.

Schematic of the standard vaporizer (SV) and capture vaporizer (CV) and setup for different sampling system; comparison of O:C and H:C from argon and air systems; exploration of the impact of alternative fragmentation tables for CO^+ and H_2O^+ for ambient measurements with the CV; calibrated O:C and H:C ratios of ambient OA between CV versus SV; scatter plot between calibrated O: C values and f_{44} and calibrated H:C values and f_{43}; dependence of key OA parameters on particle beam position on the CV; MS spectra of the PMF factors for the three-factor solution of the CV data set with different FPEAK for KORUS-AQ study; correlation coefficient (R) between the timeseries of PMF factors with different external tracers for the KORUS-AQ campaign (RF-05); (a) scatter plots of f_{44} in different PMF factors during the three field studies; scatter plots of (b) O:C and (c) H:C ratios in PMF factors during the KORUS-AQ study; m/z-dependent average signal-to-noise ratio (S/N) from both the SV and CV during the three field studies; Table S1 showing information about the pure standard species sampled in the CV in Figure 8; information about the pure standard species sampled in the SV in Figure 1; comparison of organic CO^+/CO_2^+ and organic H_2O^+/CO_2^+ between the CV and SV; and uncertainties calculated for each PMF factor using the bootstraping method (PDF)

■ AUTHOR INFORMATION

Corresponding Author

*E-mail for J.L.J.: jose.jimenez@colorado.edu.

DOI: 10.1021/acsearthspacechem.8b00002
ACS Earth Space Chem. 2018, 2, 410−421

Present address

[#]State Key Laboratory of Organic Geochemistry and Guangdong Key Laboratory of Environment Protection and Resources Utilization, Guangzhou Institute of Geochemistry, Chinese Academy of Sciences, Guangzhou 510640, China.

ORCID

Weiwei Hu: 0000-0002-3485-6304
Taehyun Park: 0000-0002-1030-7618
Jose L. Jimenez: 0000-0001-6203-1847

Notes

The authors declare no competing financial interest.

■ ACKNOWLEDGMENTS

This research was partially supported by NASA NNX15AT96G, NSF AGS-1243354, DOE (BER/ASR) DE-SC0016559, and a CIRES IRP grant. Development of the Capture Vaporizer device was supported by the U.S. Department of Energy SBIR program DE-SC0001673. We sincerely thank Uwe Karst, Tim Elseberg, and Teledyne CETAC for the use of the laser ablation setup for our experiment. We thank the DC-8 crew for their help and support during the KORUS-AQ study and the DC-8 science team for the use of their data for identifying the PMF factors.

■ ABBREVIATION/GLOSSARY/NOMENCLATURE

ACSM	Aerosol chemical speciation monitor
A-A method	Aiken ambient method
A-E method	Aiken explicit method
AMS	Aerosol mass spectrometer
ARI	Aerodyne research incorporated.
BB	Biomass burning
BBOA	Biomass burning organic aerosol
CE	Collection efficiency
C-IA method	Canagaratna Improved-Ambient method
CPC	Condensation particle counter
C-ToF-MS	Compact time-of-flight mass spectrometer
CMB	Chemical mass balance
CV	Capture vaporizer
CV-AMS	Aerosol mass spectrometer equipped with a capture vaporizer
DMA	Differential mobility analyzer
f_{CO2}	The ratio of the organic CO_2^+ signal to the total OA signal
f_{44}	The ratio of the m/z 44 signal to the total OA signal
f_{43}	The ratio of the m/z 43 signal to the total OA signal
$f_{m/z}$	The ratio of the organic signal at a given m/z to the total OA signal
FPEAK	A parameter used to explore the rotational freedom of solution in positive matrix factorization analysis.
H:C	Hydrogen-to-carbon atomic ratio of OA
HR	High resolution
HR-ToF-MS	High-resolution time-of-flight mass spectrometer
HR-ToF-AMS	High-resolution time-of-flight aerosol mass spectrometer
HOA	Hydrocarbon-like organic aerosol
IE	Ionization efficiency
IEPOX-SOA	Isoprene derived epoxydiols secondary organic aerosol, which is SOA mainly formed from isoprene oxidation under low NO condition.
IGOR pro	An interactive software environment for analysis of scientific and engineering data and the production of publication-quality graphs.
KORUS-AQ	KORean-United States Air Quality mission, a aircraft study carried out in and around South Korea.
LO-OOA	Less-oxidized oxygenated organic aerosol
LToF-AMS	Long time-of-flight aerosol mass spectrometer, which has a resolution approaching 8000 m/Δm
MS	Mass spectrometer
ME-2	Multilinear engine, a software tool that can perform constrained PMF analysis
MO-OOA	More-oxidized oxygenated organic aerosol
N:C	Nitrogen-to-carbon atomic ratio of OA
Nd: YAG	Neodymium-doped yttrium aluminum garnet; $Nd:Y_3Al_5O_{12}$, which is a crystal that is used as a lasing medium for solid-state lasers.
NH_4NO_3	Ammonium nitrate
$(NH_4)_2SO_4$.	Ammonium sulfate
NO_3 radical	Nitrate radical
NOx	Nitrogen oxides (=NO_2+NO)
O_3	Ozone
OA	Organic aerosol
OOA	Oxygenated organic aerosol
OA:OC	Organic aerosol to organic carbon ratio
OC	Organic carbon
O:C	Oxygen-to-carbon atomic ratio of OA
OM:OC	Organic matter to organic carbon ratio, which is equal to OA:OC
OSc	Average carbon oxidation state
PET	PMF Evolution Tool, an interface using IGOR pro software for unconstrained PMF analysis (developed by the Jimenez group at the university of Colorado)
PMF	Positive matrix factorization,
PCI	Pressure controlled inlet
Q/Q_{exp}	Ratio of the weighted squared residual ("Q") to the expected value, if the PMF model applied and the error are correctly specified. This parameter is used to evaluate PMF results.
RH	Relative humidity
SMPS	Scanning mobility particle sizer
SOA	Secondary organic aerosol
SOAS	Southern oxidant and aerosol study, a field study carried out in the southeastern US in summer 2013.
SoFi	A interface IGOR software developed by Paul Scherrer Institute for constrained PMF (ME-2) analysis
S/N	Signal-to-noise
SV	Standard vaporizer
SV-AMS	Aerosol mass spectrometer equipped with a standard vaporizer
TLC	Thin-layer chromatography
UMR	Unit mass resolution

■ REFERENCES

(1) Canagaratna, M. R.; Jayne, J. T.; Jimenez, J. L.; Allan, J. D.; Alfarra, M. R.; Zhang, Q.; Onasch, T. B.; Drewnick, F.; Coe, H.; Middlebrook, A.; Delia, A.; Williams, L. R.; Trimborn, A. M.;

DOI: 10.1021/acsearthspacechem.8b00002
ACS Earth Space Chem. 2018, 2, 410−421

Northway, M. J.; DeCarlo, P. F.; Kolb, C. E.; Davidovits, P.; Worsnop, D. R. Chemical and microphysical characterization of ambient aerosols with the aerodyne aerosol mass spectrometer. *Mass Spectrom. Rev.* **2007**, *26* (2), 185−222.
(2) Jayne, J. T.; Leard, D. C.; Zhang, X. F.; Davidovits, P.; Smith, K. A.; Kolb, C. E.; Worsnop, D. R. Development of an aerosol mass spectrometer for size and composition analysis of submicron particles. *Aerosol Sci. Technol.* **2000**, *33* (1−2), 49−70.
(3) Kimmel, J. R.; Farmer, D. K.; Cubison, M. J.; Sueper, D.; Tanner, C.; Nemitz, E.; Worsnop, D. R.; Gonin, M.; Jimenez, J. L. Real-time aerosol mass spectrometry with millisecond resolution. *Int. J. Mass Spectrom.* **2011**, *303* (1), 15−26.
(4) Ng, N. L.; Jayne, J. T.; Herndon, S. C.; Trimborn, A.; Canagaratna, M. R.; Croteau, P. L.; Onasch, T. B.; Sueper, D.; Worsnop, D. R.; Zhang, Q.; Sun, Y. L. An Aerosol Chemical Speciation Monitor (ACSM) for Routine Monitoring of the Composition and Mass Concentrations of Ambient Aerosol. *Aerosol Sci. Technol.* **2011**, *45* (7), 780−794.
(5) Ulbrich, I. M.; Canagaratna, M. R.; Zhang, Q.; Worsnop, D. R.; Jimenez, J. L. Interpretation of organic components from Positive Matrix Factorization of aerosol mass spectrometric data. *Atmos. Chem. Phys.* **2009**, *9* (9), 2891−2918.
(6) Canonaco, F.; Crippa, M.; Slowik, J. G.; Baltensperger, U.; Prévôt, A. S. H. SoFi, an IGOR-based interface for the efficient use of the generalized multilinear engine (ME-2) for the source apportionment: ME-2 application to aerosol mass spectrometer data. *Atmos. Meas. Tech.* **2013**, *6* (12), 3649−3661.
(7) Lanz, V. A.; Alfarra, M. R.; Baltensperger, U.; Buchmann, B.; Hueglin, C.; Prevot, A. S. H. Source apportionment of submicron organic aerosols at an urban site by factor analytical modelling of aerosol mass spectra. *Atmos. Chem. Phys.* **2007**, *7* (6), 1503−1522.
(8) Zhang, Q.; Alfarra, M. R.; Worsnop, D. R.; Allan, J. D.; Coe, H.; Canagaratna, M. R.; Jimenez, J. L. Deconvolution and quantification of hydrocarbon-like and oxygenated organic aerosols based on aerosol mass spectrometry. *Environ. Sci. Technol.* **2005**, *39* (13), 4938−4952.
(9) Crippa, M.; El Haddad, I.; Slowik, J. G.; DeCarlo, P. F.; Mohr, C.; Heringa, M. F.; Chirico, R.; Marchand, N.; Sciare, J.; Baltensperger, U.; Prévôt, A. S. H. Identification of marine and continental aerosol sources in Paris using high resolution aerosol mass spectrometry. *Journal of Geophysical Research: Atmospheres* **2013**, *118*, 1950−1963.
(10) Fröhlich, R.; Crenn, V.; Setyan, A.; Belis, C. A.; Canonaco, F.; Favez, O.; Riffault, V.; Slowik, J. G.; Aas, W.; Aijälä, M.; Alastuey, A.; Artiñano, B.; Bonnaire, N.; Bozzetti, C.; Bressi, M.; Carbone, C.; Coz, E.; Croteau, P. L.; Cubison, M. J.; Esser-Gietl, J. K.; Green, D. C.; Gros, V.; Heikkinen, L.; Herrmann, H.; Jayne, J. T.; Lunder, C. R.; Minguillón, M. C.; Močnik, G.; O'Dowd, C. D.; Ovadnevaite, J.; Petralia, E.; Poulain, L.; Priestman, M.; Ripoll, A.; Sarda-Estève, R.; Wiedensohler, A.; Baltensperger, U.; Sciare, J.; Prévôt, A. S. H. ACTRIS ACSM intercomparison − Part 2: Intercomparison of ME-2 organic source apportionment results from 15 individual, co-located aerosol mass spectrometers. *Atmos. Meas. Tech.* **2015**, *8* (6), 2555−2576.
(11) Canagaratna, M. R.; Jimenez, J. L.; Kroll, J. H.; Chen, Q.; Kessler, S. H.; Massoli, P.; Hildebrandt Ruiz, L.; Fortner, E.; Williams, L. R.; Wilson, K. R.; Surratt, J. D.; Donahue, N. M.; Jayne, J. T.; Worsnop, D. R. Elemental ratio measurements of organic compounds using aerosol mass spectrometry: characterization, improved calibration, and implications. *Atmos. Chem. Phys.* **2015**, *15* (1), 253−272.
(12) Aiken, A. C.; Decarlo, P. F.; Kroll, J. H.; Worsnop, D. R.; Huffman, J. A.; Docherty, K. S.; Ulbrich, I. M.; Mohr, C.; Kimmel, J. R.; Sueper, D.; Sun, Y.; Zhang, Q.; Trimborn, A.; Northway, M.; Ziemann, P. J.; Canagaratna, M. R.; Onasch, T. B.; Alfarra, M. R.; Prevot, A. S. H.; Dommen, J.; Duplissy, J.; Metzger, A.; Baltensperger, U.; Jimenez, J. L. O/C and OM/OC ratios of primary, secondary, and ambient organic aerosols with high-resolution time-of-flight aerosol mass spectrometry. *Environ. Sci. Technol.* **2008**, *42* (12), 4478−4485.
(13) Jimenez, J. L.; Canagaratna, M. R.; Donahue, N. M.; Prevot, A. S. H.; Zhang, Q.; Kroll, J. H.; DeCarlo, P. F.; Allan, J. D.; Coe, H.; Ng, N. L.; Aiken, A. C.; Docherty, K. S.; Ulbrich, I. M.; Grieshop, A. P.; Robinson, A. L.; Duplissy, J.; Smith, J. D.; Wilson, K. R.; Lanz, V. A.; Hueglin, C.; Sun, Y. L.; Tian, J.; Laaksonen, A.; Raatikainen, T.; Rautiainen, J.; Vaattovaara, P.; Ehn, M.; Kulmala, M.; Tomlinson, J. M.; Collins, D. R.; Cubison, M. J.; Dunlea, E. J.; Huffman, J. A.; Onasch, T. B.; Alfarra, M. R.; Williams, P. I.; Bower, K.; Kondo, Y.; Schneider, J.; Drewnick, F.; Borrmann, S.; Weimer, S.; Demerjian, K.; Salcedo, D.; Cottrell, L.; Griffin, R.; Takami, A.; Miyoshi, T.; Hatakeyama, S.; Shimono, A.; Sun, J. Y.; Zhang, Y. M.; Dzepina, K.; Kimmel, J. R.; Sueper, D.; Jayne, J. T.; Herndon, S. C.; Trimborn, A. M.; Williams, L. R.; Wood, E. C.; Middlebrook, A. M.; Kolb, C. E.; Baltensperger, U.; Worsnop, D. R. Evolution of Organic Aerosols in the Atmosphere. *Science* **2009**, *326* (5959), 1525−1529.
(14) Kroll, J. H.; Donahue, N. M.; Jimenez, J. L.; Kessler, S. H.; Canagaratna, M. R.; Wilson, K. R.; Altieri, K. E.; Mazzoleni, L. R.; Wozniak, A. S.; Bluhm, H.; Mysak, E. R.; Smith, J. D.; Kolb, C. E.; Worsnop, D. R. Carbon oxidation state as a metric for describing the chemistry of atmospheric organic aerosol. *Nat. Chem.* **2011**, *3* (2), 133−139.
(15) Heald, C. L.; Kroll, J. H.; Jimenez, J. L.; Docherty, K. S.; DeCarlo, P. F.; Aiken, A. C.; Chen, Q.; Martin, S. T.; Farmer, D. K.; Artaxo, P. A simplified description of the evolution of organic aerosol composition in the atmosphere. *Geophys. Res. Lett.* **2010**, *37*, L08803.
(16) Ng, N. L.; Canagaratna, M. R.; Jimenez, J. L.; Chhabra, P. S.; Seinfeld, J. H.; Worsnop, D. R. Changes in organic aerosol composition with aging inferred from aerosol mass spectra. *Atmos. Chem. Phys.* **2011**, *11* (13), 6465−6474.
(17) Philip, S.; Martin, R. V.; Pierce, J. R.; Jimenez, J. L.; Zhang, Q.; Canagaratna, M. R.; Spracklen, D. V.; Nowlan, C. R.; Lamsal, L. N.; Cooper, M. J.; Krotkov, N. A. Spatially and seasonally resolved estimate of the ratio of organic mass to organic carbon. *Atmos. Environ.* **2014**, *87*, 34−40.
(18) Chen, Q.; Liu, Y.; Donahue, N. M.; Shilling, J. E.; Martin, S. T. Particle-Phase Chemistry of Secondary Organic Material: Modeled Compared to Measured O: C and H: C Elemental Ratios Provide Constraints. *Environ. Sci. Technol.* **2011**, *45* (11), 4763−4770.
(19) Chen, Q.; Heald, C. L.; Jimenez, J. L.; Canagaratna, M. R.; Zhang, Q.; He, L.-Y.; Huang, X.-F.; Campuzano-Jost, P.; Palm, B. B.; Poulain, L.; Kuwata, M.; Martin, S. T.; Abbatt, J. P. D.; Lee, A. K. Y.; Liggio, J. Elemental composition of organic aerosol: The gap between ambient and laboratory measurements. *Geophys. Res. Lett.* **2015**, *42* (10), 4182−4189.
(20) Dzepina, K.; Jimenez, J. L.; Cappa, C. D.; Volkamer, R. M.; Madronich, S.; DeCarlo, P. F.; Zaveri, R. A. Modeling the Multiday Evolution and Aging of Secondary Organic Aerosol During MILAGRO 2006. *Environ. Sci. Technol.* **2011**, *45* (8), 3496−3503.
(21) Dzepina, K.; Volkamer, R. M.; Madronich, S.; Tulet, P.; Ulbrich, I. M.; Zhang, Q.; Cappa, C. D.; Ziemann, P. J.; Jimenez, J. L. Evaluation of recently-proposed secondary organic aerosol models for a case study in Mexico City. *Atmos. Chem. Phys.* **2009**, *9* (15), 5681−5709.
(22) Waxman, E. M.; Dzepina, K.; Ervens, B.; Lee-Taylor, J.; Aumont, B.; Jimenez, J. L.; Madronich, S.; Volkamer, R. Secondary organic aerosol formation from semi- and intermediate-volatility organic compounds and glyoxal: Relevance of O/C as a tracer for aqueous multiphase chemistry. *Geophys. Res. Lett.* **2013**, *40*, 978−982.
(23) Middlebrook, A. M.; Bahreini, R.; Jimenez, J. L.; Canagaratna, M. R. Evaluation of Composition-Dependent Collection Efficiencies for the Aerodyne Aerosol Mass Spectrometer using Field Data. *Aerosol Sci. Technol.* **2012**, *46* (3), 258−271.
(24) Matthew, B. M.; Middlebrook, A. M.; Onasch, T. B. Collection efficiencies in an Aerodyne Aerosol Mass Spectrometer as a function of particle phase for laboratory generated aerosols. *Aerosol Sci. Technol.* **2008**, *42* (11), 884−898.
(25) Bahreini, R.; Ervens, B.; Middlebrook, A. M.; Warneke, C.; de Gouw, J. A.; DeCarlo, P. F.; Jimenez, J. L.; Brock, C. A.; Neuman, J. A.; Ryerson, T. B.; Stark, H.; Atlas, E.; Brioude, J.; Fried, A.; Holloway, J. S.; Peischl, J.; Richter, D.; Walega, J.; Weibring, P.; Wollny, A. G.; Fehsenfeld, F. C. Organic aerosol formation in urban and industrial

DOI: 10.1021/acsearthspacechem.8b00002
ACS Earth Space Chem. 2018, 2, 410−421

plumes near Houston and Dallas, Texas. *J. Geophys. Res.* **2009**, *114* (D7), D00F16.
(26) Jayne, J. T.; Worsnop, D. R. Particle capture device. Aerodyne Research, Inc.; Patent Application 20150040689A1, 2016.
(27) Hu, W.; Campuzano-Jost, P.; Day, D. A.; Croteau, P.; Canagaratna, M. R.; Jayne, J. T.; Worsnop, D. R.; Jimenez, J. L. Evaluation of the new capture vaporizer for aerosol mass spectrometers (AMS) through field studies of inorganic species. *Aerosol Sci. Technol.* **2017**, *51* (6), 735−754.
(28) Hu, W.; Campuzano-Jost, P.; Day, D. A.; Croteau, P.; Canagaratna, M. R.; Jayne, J. T.; Worsnop, D. R.; Jimenez, J. L. Evaluation of the new capture vapourizer for aerosol mass spectrometers (AMS) through laboratory studies of inorganic species. *Atmos. Meas. Tech.* **2017**, *10* (8), 2897−2921.
(29) Xu, W.; Croteau, P.; Williams, L.; Canagaratna, M.; Onasch, T.; Cross, E.; Zhang, X.; Robinson, W.; Worsnop, D.; Jayne, J. Laboratory characterization of an aerosol chemical speciation monitor with PM2.5 measurement capability. *Aerosol Sci. Technol.* **2017**, *51* (1), 69−83.
(30) Hu, W. W.; Campuzano-Jost, P.; Day, D. A.; Nault, B. A.; Park, T.; Lee, T.; Croteau, P. L.; Canagaratna, M. R.; Jayne, J. T.; Jimenez, J. L. Evaluation of the new capture vaporizer for Aerosol Mass Spectrometers (AMS): characterization of organic aerosol (OA) mass spectra. *Aerosol Sci. Technol.* **2018**, accepted.
(31) Gunther, D.; Heinrich, C. A. Enhanced sensitivity in laser ablation-ICP mass spectrometry using helium-argon mixtures as aerosol carrier. *J. Anal. At. Spectrom.* **1999**, *14* (9), 1363−1368.
(32) Reifschneider, O.; Wentker, K. S.; Strobel, K.; Schmidt, R.; Masthoff, M.; Sperling, M.; Faber, C.; Karst, U. Elemental Bioimaging of Thulium in Mouse Tissues by Laser Ablation-ICPMS as a Complementary Method to Heteronuclear Proton Magnetic Resonance Imaging for Cell Tracking Experiments. *Anal. Chem.* **2015**, *87* (8), 4225−4230.
(33) Berry, J. L.; Day, D. A.; Elseberg, T.; Palm, B. B.; Hu, W.; Abdelhamid, A.; Schroder, J. C.; Karst, U.; Jimenez, J. L.; Browne, E. C. Laser ablation-aerosol mass spectrometry-chemical ionization mass spectrometry for ambient imaging. *Anal. Chem.* **2018**, in press. DOI: 10.1021/acs.analchem.7b05255.
(34) Aimanant, S.; Ziemann, P. J. Chemical Mechanisms of Aging of Aerosol Formed from the Reaction of n-Pentadecane with OH Radicals in the Presence of NOx. *Aerosol Sci. Technol.* **2013**, *47* (9), 979−990.
(35) Carlton, A. M.; de Gouw, J.; Jimenez, J. L.; Ambrose, J. L.; Brown, S.; Baker, K. R.; Brock, C. A.; Cohen, R. C.; Edgerton, S.; Farkas, C.; Farmer, D.; Goldstein, A. H.; Gratz, L.; Guenther, A.; Hunt, S.; Jaeglé, L.; Jaffe, D. A.; Mak, J.; McClure, C.; Nenes, A.; Nguyen, T. K. V.; Pierce, J. R.; Selin, N.; Shah, V.; Shaw, S.; Shepson, P. B.; Song, S.; Stutz, J.; Surratt, J.; Turpin, B. J.; Warneke, C.; Washenfelder, R. A.; Wennberg, P. O.; Zhou, X. The Southeast Atmosphere Studies (SAS): coordinated investigation and discovery to answer critical questions about fundamental atmospheric processes. *Bull. Am. Met. Soc.* **2018**, in press.
(36) Hu, W. W.; Campuzano-Jost, P.; Palm, B. B.; Day, D. A.; Ortega, A. M.; Hayes, P. L.; Krechmer, J. E.; Chen, Q.; Kuwata, M.; Liu, Y. J.; de Sá, S. S.; McKinney, K.; Martin, S. T.; Hu, M.; Budisulistiorini, S. H.; Riva, M.; Surratt, J. D.; St. Clair, J. M.; Isaacman-Van Wertz, G.; Yee, L. D.; Goldstein, A. H.; Carbone, S.; Brito, J.; Artaxo, P.; de Gouw, J. A.; Koss, A.; Wisthaler, A.; Mikoviny, T.; Karl, T.; Kaser, L.; Jud, W.; Hansel, A.; Docherty, K. S.; Alexander, M. L.; Robinson, N. H.; Coe, H.; Allan, J. D.; Canagaratna, M. R.; Paulot, F.; Jimenez, J. L. Characterization of a real-time tracer for isoprene epoxydiols-derived secondary organic aerosol (IEPOX-SOA) from aerosol mass spectrometer measurements. *Atmos. Chem. Phys.* **2015**, *15* (20), 11807−11833.
(37) Xu, L.; Guo, H.; Boyd, C. M.; Klein, M.; Bougiatioti, A.; Cerully, K. M.; Hite, J. R.; Isaacman-VanWertz, G.; Kreisberg, N. M.; Knote, C.; Olson, K.; Koss, A.; Goldstein, A. H.; Hering, S. V.; de Gouw, J.; Baumann, K.; Lee, S.-H.; Nenes, A.; Weber, R. J.; Ng, N. L. Effects of anthropogenic emissions on aerosol formation from isoprene and monoterpenes in the southeastern United States. *Proc. Natl. Acad. Sci. U. S. A.* **2015**, *112*, 37−42.
(38) Drewnick, F.; Hings, S. S.; DeCarlo, P.; Jayne, J. T.; Gonin, M.; Fuhrer, K.; Weimer, S.; Jimenez, J. L.; Demerjian, K. L.; Borrmann, S.; Worsnop, D. R. A new time-of-flight aerosol mass spectrometer (TOF-AMS) - Instrument description and first field deployment. *Aerosol Sci. Technol.* **2005**, *39* (7), 637−658.
(39) Aiken, A. C.; DeCarlo, P. F.; Jimenez, J. L. Elemental analysis of organic species with electron ionization high-resolution mass spectrometry. *Anal. Chem.* **2007**, *79* (21), 8350−8358.
(40) DeCarlo, P. F.; Kimmel, J. R.; Trimborn, A.; Northway, M. J.; Jayne, J. T.; Aiken, A. C.; Gonin, M.; Fuhrer, K.; Horvath, T.; Docherty, K. S.; Worsnop, D. R.; Jimenez, J. L. Field-deployable, high-resolution, time-of-flight aerosol mass spectrometer. *Anal. Chem.* **2006**, *78* (24), 8281−8289.
(41) Paatero, P. Least squares formulation of robust non-negative factor analysis. *Chemom. Intell. Lab. Syst.* **1997**, *37* (1), 23−35.
(42) Paatero, P.; Tapper, U. Positive matrix factorization: A non-negative factor model with optimal utilization of error estimates of data values. *Environmetrics* **1994**, *5* (2), 111−126.
(43) Surratt, J. D.; Chan, A. W. H.; Eddingsaas, N. C.; Chan, M.; Loza, C. L.; Kwan, A. J.; Hersey, S. P.; Flagan, R. C.; Wennberg, P. O.; Seinfeld, J. H. Reactive intermediates revealed in secondary organic aerosol formation from isoprene. *Proc. Natl. Acad. Sci. U. S. A.* **2010**, *107* (15), 6640−6645.
(44) Ayres, B. R.; Allen, H. M.; Draper, D. C.; Brown, S. S.; Wild, R. J.; Jimenez, J. L.; Day, D. A.; Campuzano-Jost, P.; Hu, W.; de Gouw, J.; Koss, A.; Cohen, R. C.; Duffey, K. C.; Romer, P.; Baumann, K.; Edgerton, E.; Takahama, S.; Thornton, J. A.; Lee, B. H.; Lopez-Hilfiker, F. D.; Mohr, C.; Wennberg, P. O.; Nguyen, T. B.; Teng, A.; Goldstein, A. H.; Olson, K.; Fry, J. L. Organic nitrate aerosol formation via NO3 + biogenic volatile organic compounds in the southeastern United States. *Atmos. Chem. Phys.* **2015**, *15* (23), 13377−13392.
(45) Paatero, P. The Multilinear Engine—A Table-Driven, Least Squares Program for Solving Multilinear Problems, Including the n-Way Parallel Factor Analysis Model. *Journal of Computational and Graphical Statistics* **1999**, *8* (4), 854−888.
(46) Hu, W.; Handschy, A.; Jimenez, J. L. *AMS Capture Vaporizer Spectral Database*. See the following: http://cires1.colorado.edu/jimenez-group/AMSsd_CV/ (accessed Feb. 21, 2018).

DOI: 10.1021/acsearthspacechem.8b00002
ACS Earth Space Chem. 2018, 2, 410−421